J Mol Model (2011) 17:2005–2016
DOI 10.1007/s00894-010-0910-6

ORIGINAL PAPER

All-electron scalar relativistic calculation of water molecule adsorption onto small gold clusters

Xiang-jun Kuang · Xin-qiang Wang · Gao-bin Liu

Received: 27 May 2010 / Accepted: 21 November 2010 / Published online: 8 December 2010

Abstract An all-electron scalar relativistic calculation was performed on Au_nH_2O (n=1–13) clusters using density functional theory (DFT) with the generalized gradient approximation at PW91 level. The calculation results reveal that, after adsorption, the small gold cluster would like to bond with oxygen and the H_2O molecule prefers to occupy the single fold coordination site. Reflecting the strong scalar relativistic effect, Au_n geometries are distorted slightly but still maintain a planar structure. The Au–Au bond is strengthened and the H–O bond is weakened, as manifested by the shortening of the Au–Au bond-length and the lengthening of the H–O bond-length. The H–O–H bond angle becomes slightly larger. The enhancement of reactivity of the H_2O molecule is obvious. The Au–O bond-lengths, adsorption energies, VIPs, HLGs, HOMO (LUMO) energy levels, charge transfers and the highest vibrational frequencies of the Au–O mode for Au_nH_2O clusters exhibit an obvious odd-even oscillation. The most favorable adsorption between small gold clusters and the H_2O molecule takes place when the H_2O molecule is adsorbed onto an even-numbered Au_n cluster and becomes an Au_nH_2O cluster with an even number of valence electrons. The odd–even alteration of magnetic moments is observed in Au_nH_2O clusters and may serve as material with a tunable code capacity of "0" and "1" by adsorbing a H_2O molecule onto an odd or even-numbered small gold cluster.

Keywords Small gold cluster · Water molecule · Adsorption · All-electron scalar relativistic calculation

PACS 73.22.-f · 36.40.Cg · 36.40.Ei

X.-j. Kuang (✉) · X.-q. Wang (✉) · G.-b. Liu
College of Physics, Chongqing University,
Chongqing 400044, China
e-mail: kuangxiangjun@163.com

X.-q. Wang
e-mail: xqwang@cqu.edu.cn

X.-j. Kuang
School of Science,
Southwest University of Science and Technology,
Mianyang, Sichuan 621010, China

Introduction

Water adsorption onto metal surfaces is one of the fundamental topics in surface science, and is considered relevant to the better understanding of surface phenomena such as heterogeneous catalysis, corrosion of materials and surface electrochemistry [1–8]. Theoretical investigations of adsorption behavior in catalysis mechanisms are difficult to perform, primarily because the reactions involved occur only at infinite surfaces. This required researchers to find compromises between solid state physics and molecular physics. One common solution is to use metal clusters as models for infinite metal surfaces, and this has been used in numerous theoretical investigations into atomic and molecular adsorption in metallic systems [9–11].

Among various metal clusters, nano-sized gold clusters have attracted much attention from both industrial and scientific areas due to their unique physical and chemical properties, which are strongly dependent on cluster size [12–14]. Although bulk gold is one of the most chemically inert metals, gold clusters—the size of which can be as small as 2–3 nm—are efficient catalysts for various chemical reactions [15–18]. Previous studies have reported that nano-sized gold catalysts can be applied to many oxidation and hydrogenation reactions at low temperatures. These reactions include CO and NO oxidations [19], partial oxidation of propylene [20], partial hydrogenation of

acetylene [21], hydrogenation of ethylene [22], and so on. Indeed, there are some studies on the adsorption behavior of water molecules surrounding gold nanoparticles of different sizes or inside a gold nanotube [23–25]. Ju [23] performed a molecular dynamics simulation to investigate the adsorption of water molecules surrounding gold nanoparticles of various sizes in a parallel computing environment. Observation of the distribution of oxygen and hydrogen atoms shows that the adsorption of water molecules creates two shell-like formations of water in close vicinity to the gold nanoparticle surface. These shell-like formations are found to be more pronounced around smaller gold nanoparticles. The rearrangement of water molecules in this region reduces the local hydrogen bond strength. Chang et al. [24] also performed a molecular dynamics simulation to investigate the adsorption mechanism of water molecules surrounding gold nanoparticles of different sizes. For larger gold nanoparticles, hydrogen bonding of water molecules adsorbed onto the surface of the gold nanoparticles are arranged in a two-dimensional structure, while those adsorbed on the edge of the surface of the gold nanoparticles are arranged in a three-dimensional structure. Water molecules that are adsorbed on the larger gold nanoparticles tend to be arranged irregularly, while those adsorbed onto the smallest gold nanoparticles tend to adopt a regular arrangement. Meanwhile, Wen et al. [25] have performed a molecular dynamics simulation to study the adsorption of water molecules inside a gold nanotube. The interaction energy of the gold nanotube wall has a direct influence on the distribution of water molecules inside the gold tube, and the numbers of hydrogen bonds per water molecule affect the orientational order parameter q. In addition, the phenomenon of a group of molecules bonded inside the tube can be observed as the number of hydrogen bonds increases.

From the overview above, we find that almost all research in this field is focused on the interaction between water molecules and gold nanoparticles or gold nanotubes; few theoretical studies are available to show the interaction between small gold clusters and water molecules. Compared with its bulk counterpart and gold nanoparticles, small gold clusters exhibit drastically different fundamental properties, which may be exploited in a variety of applications such as catalysis, chemical- and bio-detectors, advanced drug delivery systems, enhanced computing systems and optoelectronics [26]. The absolute value of interaction energy between water molecules and gold nanoparticles is reduced when the water molecules surround a nanoparticle of larger diameter [23]. This observation implies that a stronger adsorption effect might exist between smaller gold clusters and water molecules. Furthermore, a previous study [27] indicates that the reason for the preference for planar structures by gold clusters up to large size may be attributed to the scalar relativistic effect of outer shell electrons causing a shrinking of the size of the s orbital and thus enhancing s-d hybridization. Thus, it is necessary to carry out a study on the adsorption behavior of water molecules onto small gold clusters by including the scalar relativistic effect. In this paper, an all-electron scalar relativistic (AER) calculation on the interaction between water molecules and small gold clusters (n=1–13) was performed by using density functional theory (DFT) with the generalized gradient approximation at PW91 level. This study attempts to locate the ground state geometrical structures and to analyze the energy and electronic structures, magnetic properties of Au_nH_2O (n=1–13) clusters in order to obtain a qualitative understanding of the interaction between water molecules and small gold clusters.

Computational methods and cluster model

The geometrical structures and electronic properties of Au_nH_2O (n=1–13) clusters are calculated using DFT. Under the framework of DFT, the scalar relativistic effect is included for the reason described above. The numerical atomic orbitals are used in the construction of molecular orbitals. In many previous cases, as an approximation, only the outer shell atom-orbitals were employed to generate the valence orbitals, and the rest of the core orbitals were frozen. Although calculations involving the AER method are more difficult to perform due to the huge computational expense, they are generally thought to provide better accuracy than those involving only all-electron (AE) and effective core potentials. The advantages of the AER calculation over effective core potential (ECP) and AE calculations have been demonstrated by some early works [28–30]. Considering the above factors, and in order to improve calculation accuracy, we chose to carry out AER calculations and use the corresponding high quality double numeric plus (DNP) basis set despite the huge computational expense.

The PW91 form of the generalized gradient approximation (GGA) for the exchange-correlation functional is adopted in the calculations and the self-consistent field (SCF) tolerance is set at 1.0×10^{-6} eV. To accelerate the calculations, the direct inversion in iterative subspace (DIIS) approach is used, with the smearing value set at $0.005Ha$. During structure optimizations, spin is unrestricted and the symmetry of the structure has no constraints. The convergence tolerance of maximum force, energy and displacement is $0.002Ha$/Å, $1.0\times10^{-5}Ha$ and 0.005 Å, respectively. During structure relaxations, spin multiplicities are considered to be at least 2, 4 and 6 for odd-electron Au_nH_2O clusters (n=1, 3, 5, 7, 9, 11 and 13) and 1, 3, and 5 for even-electron Au_nH_2O clusters (n=2, 4, 6, 8, 10 and 12). If the total energy decreases with increasing spin multiplicity, the high spin state will be considered until the energy minimum with respect to spin

multiplicity is reached. In addition, the stability of the optimized geometry is confirmed without any imaginary frequencies by computing vibrational frequencies at same level of theory.

The choice of initial geometry is important to obtain the lowest energy structures. In this work, we obtained the initial structures by the following approaches. First, considering previous studies on the configurations of pure Au_n clusters [31–35], we optimized the structures of pure Au_n clusters using the same methods and parameters. On the basis of the optimized equilibrium geometries of pure gold clusters, we obtained the initial structures of Au_nH_2O clusters by bonding H_2O molecules directly on each possible nonequivalent site of the Au_n cluster, including three possible bonding patterns: bonding with oxygen, bonding with hydrogen, or bonding with both oxygen and hydrogen. All these initial structures are fully optimized by relaxing the atomic positions until the force acting on each atom is negligible (typically $|F_i| \leq 0.002 Ha/A^0$) and by minimizing the total energy.

In order to check the intrinsic reliability and accuracy of the computational method, we chose AuH_2O^+, Au_2, Au_3, Au_5 and Au_7 as examples to calculate some properties (the corresponding experimental data of these clusters are available) by using the AER, AE and ECP methods. From the data listed in Table 1, it can be seen that the results obtained with the AER method are clearly closer to the available experimental data [34–38] than the results obtained with the AE and ECP methods. This indicates that the AER method is more reliable and more accurate than the AE and ECP methods for the study of Au_nH_2O clusters.

Results and discussion

Geometrical structures

In order to obtain the initial geometries of Au_nH_2O clusters, we optimized pure Au_n clusters and single H_2O molecules first. The lowest energy geometries of Au_n (n=2–13) clusters shown in Fig. 1 are in good agreement with previous available works [31–35]. Then, based on these optimized lowest energy geometries, we performed an extensive lowest energy geometries search for H_2O molecule adsorption onto small gold clusters as described in Computational methods and cluster model. The lowest energy geometries of Au_nH_2O (n=1–13) clusters and some isomers that have higher energy or imaginary frequencies are also displayed in this figure. For single H_2O molecules, the calculated O–H bond-length and H–O–H bond angle, which are adapted to compare with those of H_2O after adsorption, are in good agreement with experimental values [39].

To obtain the average Au–Au bond-lengths of pure Au_n clusters and Au_nH_2O (n=1–13) clusters, all Au–Au bond-lengths of each cluster are added together and divided by the number of Au–Au bonds. The average Au–Au bond-length and Au–O, H–O bond-lengths (in angstrom) are shown in Fig. 1. From these figures, we find that the H_2O molecule prefers to occupy the single fold coordination site in all Au_nH_2O clusters. The small gold cluster prefers to bond with oxygen rather than to bond with hydrogen or with both hydrogen and oxygen. Compared with pure Au_n clusters and single H_2O molecules, the Au_n geometries in all lowest energy Au_nH_2O clusters and isomers are distorted slightly but still maintain a planar structure. This situation is believed to reflect the strong scalar relativistic effect in small gold clusters mentioned in previous studies [27], and is different from carbon monoxide adsorption onto small copper clusters, in which the most stable geometries of small copper clusters change obviously after bonding with a carbon monoxide molecule [40, 41]. The H_2O structures in all Au_nH_2O clusters are slightly perturbed, and still keep their single H_2O molecule-like structure. The bonded oxygen atom locates in the same plane as the Au_n structure for all Au_nH_2O clusters. For Au_nH_2O clusters (n=1–5), the two bonded hydrogen atoms locate to the same side of the Au_n–O plane perpendicularly, but for other Au_nH_2O clusters

Table 1 Comparison of results of all-electron scalar relativistic (AER), all-electron (AE), and effective core potential (ECP) calculations for some properties of AuH_2O^+, Au_2, Au_3, Au_5 and Au_7 clusters

Cluster	Property	AER	AE	ECP	Experimental data
AuH_2O^+	E_b (eV/atom)	1.621	1.424	1.595	1.649
Au_2	R (nm)	0.2487	0.2780	0.2624	0.2470
	E_b (eV/atom)	1.210	0.7657	0.9476	1.150
	VIP(eV)	9.370	7.3149	9.2052	9.500
	$\nu(cm^{-1})$	183.1	122.6	158.0	191.0
Au_3	VIP (eV)	7.443	5.585	7.279	7.500
Au_5		7.728	5.853	7.588	8.000
Au_7	VIP (eV)	171.1	102.9	149.2	165
	$\nu(cm^{-1})$	192.3	119.4	164.0	185
	ν (cm^{-1})	208.2	132.7	179.7	203
	$\nu(cm^{-1})$				

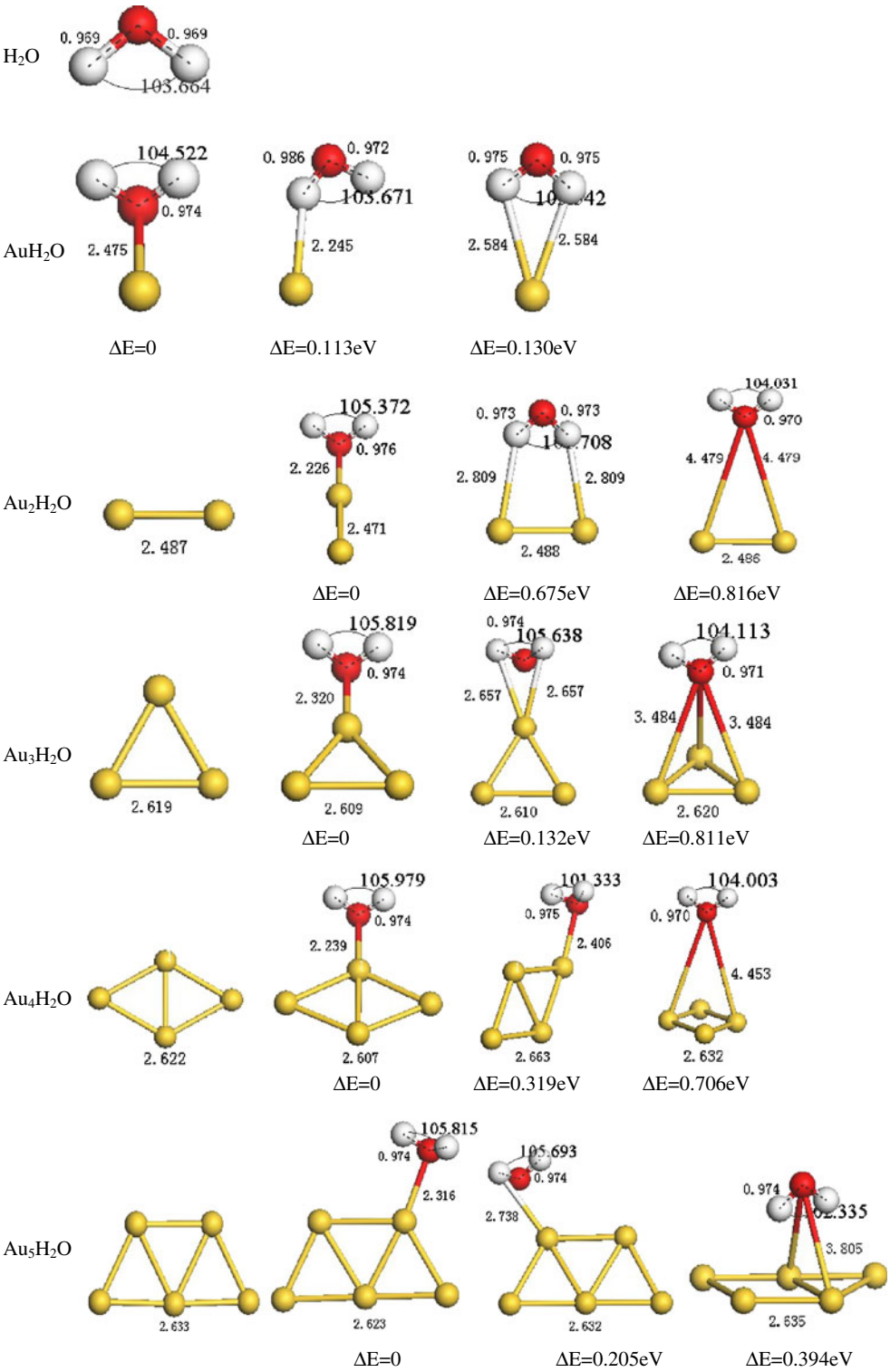

Fig. 1 Optimized geometries for pure Au_n (n=2–13) clusters, single H_2O molecules and Au_nH_2O (n=1–13) clusters. The average Au–Au bond-length, Au–O, H–O bond-lengths (in angstrom), H–O–H bond angles and energy are shown

the two bonded hydrogen atoms locate to both sides of the Au_n–O plane perpendicularly. After adsorption, the average Au–Au bond-length in the Au_nH_2O cluster is shorter than that in the corresponding pure gold cluster, and the H–O bond-lengths in all Au_nH_2O clusters are longer than the H–O bond-length in single H_2O molecules, and the H–O–H bond angle becomes larger. It is inferred that the Au–Au interaction is strengthened and the H–O interaction is weakened after adsorption. The enhancement of reactivity of H_2O molecule is obvious. This situation can be explained in terms of electron donation from the $p\pi^*$ orbital of the H_2O molecule to the $d\sigma$+sp hybridized orbital of Au, and electron

Fig. 1 (continued)

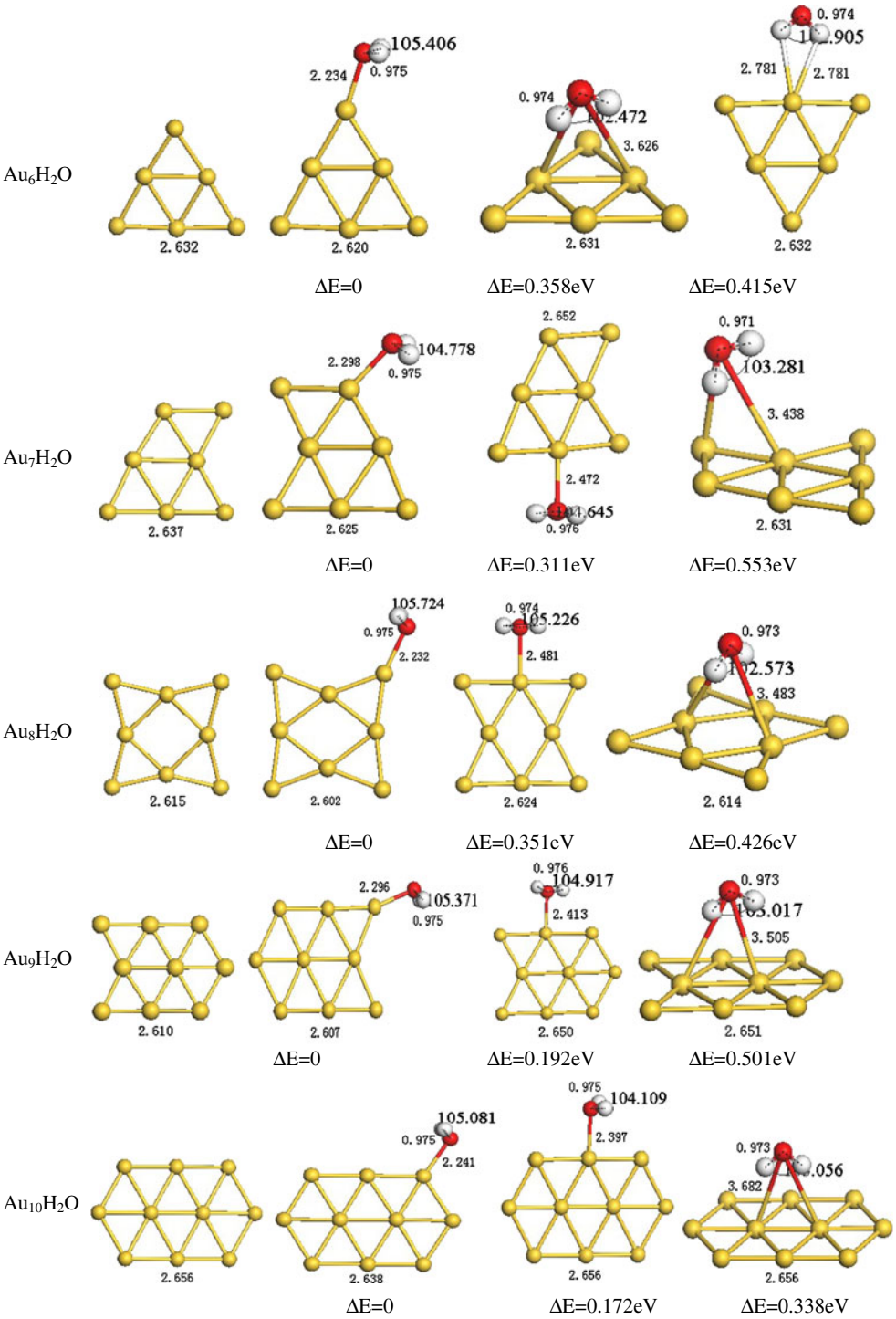

back donation from the occupied $d\pi$ orbital of Au to the unoccupied $p\pi^*$ orbital of the H_2O molecule [42], which results in better overlap between these orbitals and enhancement of the interaction between small gold clusters and H_2O molecules. Meanwhile, from Fig. 1, we can also see that the Au–O bond-length in even-numbered Au_nH_2O clusters is obviously shorter than that in adjacent odd-numbered Au_nH_2O clusters. The Au–O bond-lengths for Au_nH_2O clusters exhibit an odd-even oscillation, indicating that the Au–O interaction in even-numbered Au_nH_2O clusters is stronger than that in adjacent odd-numbered Au_nH_2O clusters.

Energy and electronic structure

The binding energies E_b, adsorption energies E_{ad}, highest occupied molecular orbital (HOMO) and lowest unoccupied

Fig. 1 (continued)

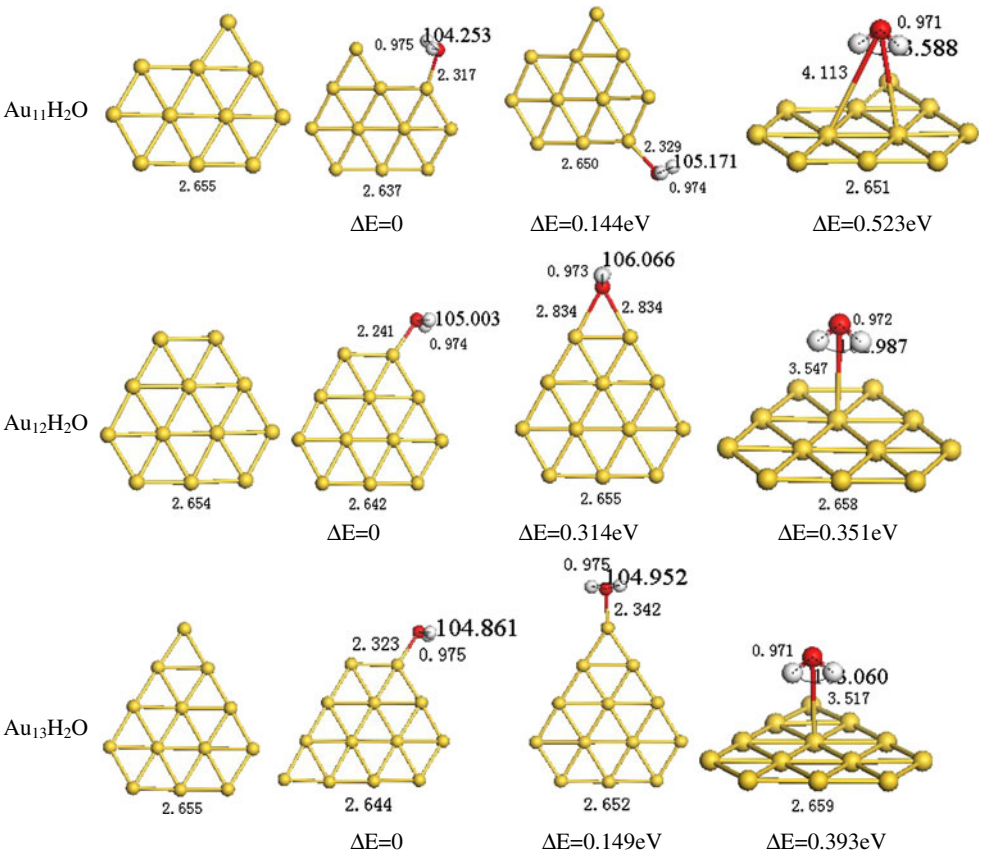

molecular orbital (LUMO) energy levels, HOMO−LUMO gaps (HLG), and vertical ionization potentials (VIP) for Au_nH_2O clusters are listed in Table 2, where we define: $E_b = [nE(Au) + E(O) + 2E(H) - E(Au_nH_2O)]/(n+3)$, $E_{ad} = [E(Au_n) + E(H_2O) - E(Au_nH_2O)]$ and $VIP = E(Au_nH_2O)^+ - E(Au_nH_2O)$, respectively. Generally speaking, the binding energy of a given cluster is a measurement of its total thermodynamic stability. From Table 2 and Fig. 2, it can be seen that the binding energy of Au_nH_2O cluster is obviously larger than that of corresponding pure gold cluster, and with the increasing number of gold atoms, the binding energy of pure gold cluster increases gradually and reaches a maximum value of 2.481 eV at n=13. Meanwhile, the binding energy of the Au_nH_2O cluster decreases gradually and reaches a minimum value of 3.543 eV at n=13 too. But, the binding energy difference between Au_nH_2O and Au_n clusters gradually becomes smaller. This indicates that the adsorption of water molecule enhances the energetic stability of pure gold cluster. With increasing number of gold atoms, the stability of Au_nH_2O cluster decreases gradually despite the increasing stability of pure gold clusters. But, the stability enhancement effect of water molecule adsorption is weakened gradually with the increasing size of the Au_nH_2O cluster.

Adsorption energy is an important index with which to examine the adsorption strength and the interaction between adsorbent and adsorbate, and has been used in some previous studies on H_2, NO and CO adsorption onto small gold clusters [42–44]. From the adsorption energies displayed in Table 2, we can see that, with increasing number of gold atoms, the adsorption energy of even-numbered Au_nH_2O cluster is larger than that of adjacent odd-numbered Au_nH_2O cluster. The odd-even oscillation of adsorption energies for Au_nH_2O clusters is clearly evident (Fig. 3). It is suggested that the adsorption strength and Au_n–H_2O interaction in even-numbered Au_nH_2O cluster are stronger than those in adjacent odd-numbered Au_nH_2O cluster. The H_2O molecule is more relatively more likely to be adsorbed by even-numbered small gold clusters. Comparing with the available data of previous studies, we find that the adsorption energy of Au_nH_2O clusters is smaller than the adsorption energy of Au_nCO clusters (n=1–6) [43] and larger than the adsorption energy of Au_nH_2 (n=1–10) [44] and Au_nNO (n=1–6) [42] clusters. This indicates that, for small gold clusters, the adsorption strength toward water molecules is weaker than the adsorption strength toward carbon monoxide molecule, and stronger than the adsorption strength toward hydrogen and nitric monoxide molecules.

Table 2 Some calculated energy data for Au_nH_2O clusters. E_b Binding energy, E_{ad} adsorption energy, *HOMO* highest occupied molecular orbital, *LUMO* lowest unoccupied molecular orbital, *HLG* HOMO−LUMO gap, *VIP* vertical ionization potential

Cluster	E_b (eV/atom)		E_{ad}	HOMO	LUMO	HLG	VIP
	Au_n	Au_nH_2O	(eV)	(eV)	(eV)	(eV)	(eV)
AuH_2O	0.000	6.054	0.354	−4.950	−4.240	0.710	8.256
Au_2H_2O	1.214	5.442	0.922	−5.311	−3.002	2.309	8.477
Au_3H_2O	1.391	4.798	0.758	−4.157	−3.588	0.569	6.659
Au_4H_2O	1.742	4.520	0.814	−5.187	−3.286	1.901	7.426
Au_5H_2O	1.925	4.251	0.516	−4.760	−4.434	0.326	6.916
Au_6H_2O	2.155	4.161	0.659	−5.230	−3.455	1.775	7.288
Au_7H_2O	2.189	3.955	0.610	−4.903	−4.666	0.237	6.831
Au_8H_2O	2.258	3.880	0.750	−5.190	−4.035	1.155	7.010
Au_9H_2O	2.293	3.758	0.605	−4.851	−4.639	0.212	6.643
$Au_{10}H_2O$	2.377	3.712	0.624	−5.322	−4.159	1.163	6.921
$Au_{11}H_2O$	2.402	3.632	0.559	−5.136	−4.966	0.170	6.784
$Au_{12}H_2O$	2.473	3.610	0.623	−5.420	−4.386	1.034	7.097
$Au_{13}H_2O$	2.481	3.543	0.568	−4.881	−4.747	0.134	6.500

The VIP is often used to investigate the chemical stability of small clusters; the larger the VIP, the deeper the HOMO energy level, which leads to less reactivity or higher chemical stability. HLG is another useful parameter for examining the electronic stability of a cluster. The larger the HLG, the higher the energy required to excite the electrons from valence band to conduction band, corresponding to higher stability of the electronic structure. From the data listed in Table 2, we find that the VIP and HLG of even-numbered Au_nH_2O cluster are larger than those of adjacent odd-numbered Au_nH_2O cluster. Meanwhile, the HOMO (LUMO) energy levels of even-numbered Au_nH_2O cluster is deeper (higher) than that of adjacent odd-numbered Au_nH_2O cluster. The VIPs, HLGs and HOMO (LUMO) energy levels of Au_nH_2O clusters show a clear odd-even oscillation (see Fig. 4). It is thought that even-numbered Au_nH_2O cluster might be more stable than the adjacent odd-numbered Au_nH_2O clusters, both electronically and chemically. This odd-even oscillation can also be observed in H-binding onto small gold clusters, and explained in terms of the electron pairing effect [45].

For any cluster, the number of electrons in the HOMO determines its ground-state electronic configuration. By orbital occupation analysis, we find that the HOMOs of even-numbered Au_nH_2O clusters with even numbers of valence electrons are fully occupied by the majority spin

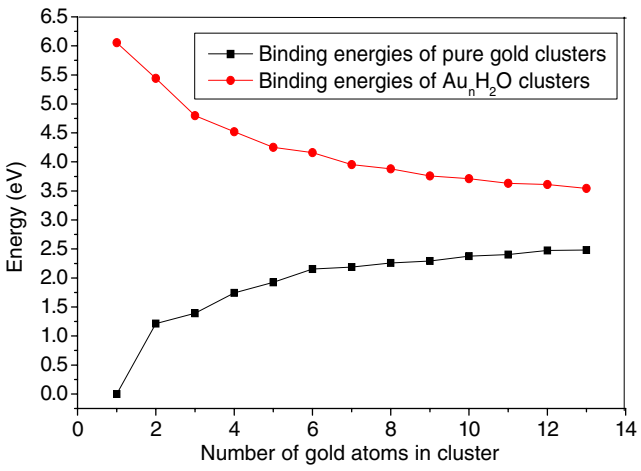

Fig. 2 Size dependence of binding energy for Au_nH_2O and Au_n clusters

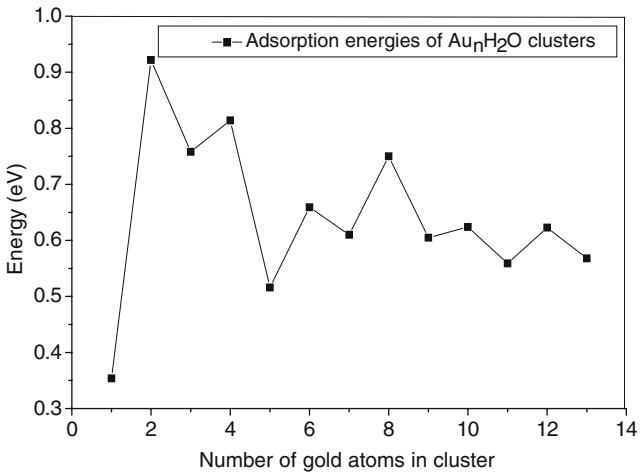

Fig. 3 Size dependence of adsorption energy for Au_nH_2O clusters

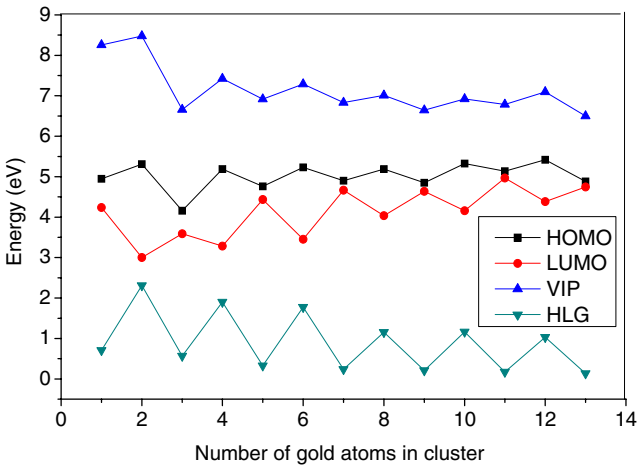

Fig. 4 Size dependence of vertical ionization potentials (VIP), HOMO−LUMO gaps (HLG), highest occupied molecular orbital (HOMO) and lowest unoccupied molecular orbital (LUMO) energy levels for Au_nH_2O clusters

and minority spin electrons, which leads to the ground state of these clusters have closed electronic shells and are remarkably stable. But, the HOMOs of odd-numbered Au_nH_2O clusters with odd number of valence electrons are occupied only partially by majority spin electrons and have open electronic shells (see Table 3). According to the Jahn-Teller theorem, these clusters have the tendency to distort further toward slower symmetry in order to reduce or remove their degeneracies and lower their energies. However, we must point out that open shell clusters may also increase their degeneracies, and that they have high spin multiplicity if the total energy is decreased. This depends on a compromise between the decrease in total energy and the increase in degeneracy. This compromise will decide whether, and to what extent, the Jahn-Teller distortion may take place [46].

The interaction between a small gold cluster and a H_2O molecule can also be reflected through charge transfers. We performed a Mulliken charge analysis of Au_nH_2O clusters and list the effective charges on Au_n, H and O in Table 3. The values of charge transfers are favorable to the mechanism of electron donation, i.e., charge transfer from the H_2O molecule to the gold cluster. Further analysis indicates that, after adsorption, the charges are transferred not only from two hydrogen atoms to the oxygen atom but also from the two hydrogen atoms to Au_n. Compared with single H_2O molecules, the value of charge transfer from two hydrogen atoms to the oxygen atom in Au_nH_2O clusters becomes small. This situation of charge transfer provides more pairing chances for electrons of Au_n and less pairing chances for electrons of H_2O. It strengthens the Au–Au bond and weakens the H–O bond, appearing as a shortening of Au–Au bond-length and a lengthening of H–O bond-length, as illustrated clearly in Fig. 1. It also favors reactivity enhancement of the water molecule. Remarkably, greater charge transfer often leads to larger adsorption energy. The charge transfer between Au_n and the H_2O molecule in even-numbered Au_nH_2O cluster with larger adsorption energy is greater than that in adjacent odd-numbered Au_nH_2O cluster with smaller adsorption energy. The charge transfers of Au_nH_2O clusters also exhibit an

Table 3 Charge transfers, electronic configuration, spin multiplicity (M) and magnetic moment for Au_nH_2O clusters

Cluster	Charge				Electronic configuration	M	Magnetic moment (μ_B)		
	Au_n	H	H	O			Au_n	H_2O	Total
H_2O		0.247	0.247	−0.494	Closed	1		0	0
AuH_2O	−0.144	0.281	0.281	−0.418	Open	2	0.910	0.090	1
Au_2H_2O	−0.183	0.300	0.300	−0.417	Closed	1	0	0	0
Au_3H_2O	−0.143	0.293	0.293	−0.443	Open	2	0.996	0.004	1
Au_4H_2O	−0.186	0.302	0.302	−0.418	Closed	1	0	0	0
Au_5H_2O	−0.136	0.292	0.292	−0.448	Open	2	0.962	0.038	1
Au_6H_2O	−0.160	0.296	0.296	−0.432	Closed	1	0	0	0
Au_7H_2O	−0.142	0.295	0.295	−0.448	Open	2	0.984	0.016	1
Au_8H_2O	−0.172	0.300	0.300	−0.428	Closed	1	0	0	0
Au_9H_2O	−0.139	0.298	0.298	−0.457	Open	2	0.985	0.015	1
$Au_{10}H_2O$	−0.164	0.294	0.294	−0.424	Closed	1	0	0	0
$Au_{11}H_2O$	−0.140	0.296	0.296	−0.452	Open	2	0.977	0.023	1
$Au_{12}H_2O$	−0.162	0.293	0.293	−0.424	Closed	1	0	0	0
$Au_{13}H_2O$	−0.150	0.296	0.296	−0.442	Open	2	0.991	0.009	1

obvious odd-even oscillation. This situation resembles that of NO adsorption onto small gold clusters [42], and indicates that the charge transfer is more favorable to H_2O molecule adsorption onto even-numbered Au_n clusters.

In order to understand the nature of chemical bonding in these systems, we plotted the spatial orientations of HOMO for Au_nH_2O clusters in Fig. 5. At first glance, the HOMOs of these clusters are obviously delocalized, with a contribution from almost all atoms in the cluster. The strong *s-d* orbital hybridization among gold atoms in HOMO is very obvious. Besides the strong *s-d* hybridization in Au atoms, *spd* hybridization between the *s* orbital of the Au atom and the *s*, *p* orbital of the H_2O molecule also exists and is very strong in most Au_nH_2O clusters. The overlap between the frontier orbitals of H and O, or cloud overlap between the $p\pi^*$ orbital of H_2O and the $d\sigma$+*sp* hybridized orbital of Au for some of the Au_nH_2O clusters are also illustrated. The unpaired electrons in the Au_n cluster will have more chance to be paired with *s* and *p* electrons of H_2O. This picture was also observed for oxygen adsorption onto small gold clusters [47], in which the $p\pi^*$ orbital of oxygen and the $d\sigma$+*sp* hybridized orbital of Au clearly overlap.

Frequency analysis

Since many experiments on the adsorption behavior of small gold clusters are based on the Fourier transform infrared spectroscopy (FTIR) method, we focused on the vibrational frequencies of different modes in the adsorption system. Table 4 lists the highest frequencies of Au–Au, Au–O, and H–O–H mode for Au_nH_2O clusters and Au–Au, and H–O–H modes for pure Au_n clusters and single H_2O molecule. It can clearly be seen that the highest vibrational frequency of Au–O mode for even-numbered Au_nH_2O cluster is higher than that of Au–O mode for odd-numbered Au_nH_2O cluster—an obvious odd-even oscillation of the highest vibrational frequencies of Au–O mode is observed (Fig. 6). This size dependence of frequencies is approximately parallel to the size dependences of adsorption energies, charge transfers, VIPs, HLGs, and HOMO energy levels (see Figs. 3, 4), again proving that the Au–O interaction in even-numbered Au_nH_2O cluster is relatively stronger than that in adjacent odd-numbered Au_nH_2O clusters. Meanwhile, we also find that the highest vibrational frequencies of the H–O–H mode for all Au_nH_2O clusters are obviously lower than the highest vibrational frequency of H–O–H mode for single H_2O molecule, and that the highest vibrational frequency of Au–Au mode for the Au_nH_2O cluster is obviously higher than that of Au–Au mode for the corresponding pure Au_n cluster. This characteristic of frequency variation indicates that, after adsorption, the Au–Au interaction is strengthened and the H–O–H interaction is weakened in all Au_nH_2O clusters, and the reactivity of the H_2O molecule is obviously enhanced. This is perfectly consistent with the shortening of Au–Au bond-length and the lengthening of O–H bond-length.

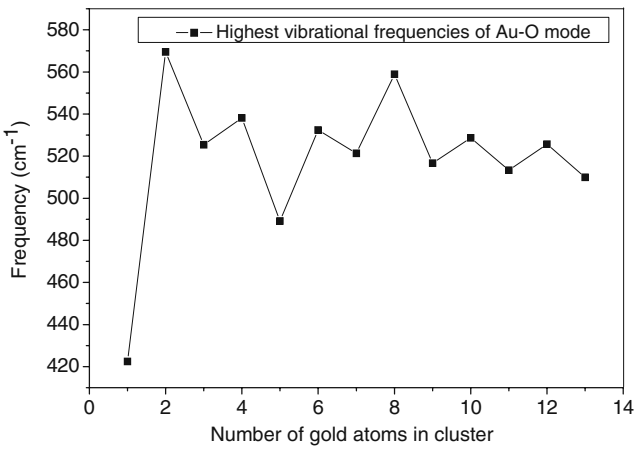

Fig. 5 Spatial orientations of HOMO for Au_nH_2O (n=1–13) clusters

Table 4 Calculated highest vibrational frequencies of Au–Au, Au–O and H–O–H modes for Au_nH_2O clusters, pure Au_n clusters and H_2O molecules

Cluster	$\nu_{Au\text{-}Au}$ (cm^{-1})	$\nu_{Au\text{-}O}$ (cm^{-1})	$\nu_{H\text{-}O\text{-}H}$ (cm^{-1})
H_2O			3,842.7
AuH_2O		422.5	3,783.4
Au_2H_2O	289.9	569.5	3,754.5
Au_2	183.1		
Au_3H_2O	275.0	525.4	3,778.8
Au_3	172.2		
Au_4H_2O	275.5	538.1	3,785.4
Au_4	174.2		
Au_5H_2O	231.9	489.2	3,781.3
Au_5	198.9		
Au_6H_2O	234.7	532.4	3,786.6
Au_6	186.0		
Au_7H_2O	253.4	521.3	3,766.0
Au_7	208.2		
Au_8H_2O	256.0	558.9	3,785.8
Au_8	220.1		
Au_9H_2O	241.7	516.7	3,782.0
Au_9	203.7		
$Au_{10}H_2O$	229.0	528.7	3,772.1
Au_{10}	199.3		
$Au_{11}H_2O$	234.1	513.3	3,746.5
Au_{11}	202.7		
$Au_{12}H_2O$	230.8	525.7	3,778.8
Au_{12}	209.0		
$Au_{13}H_2O$	232.1	509.9	3,779.5
Au_{13}	205.3		

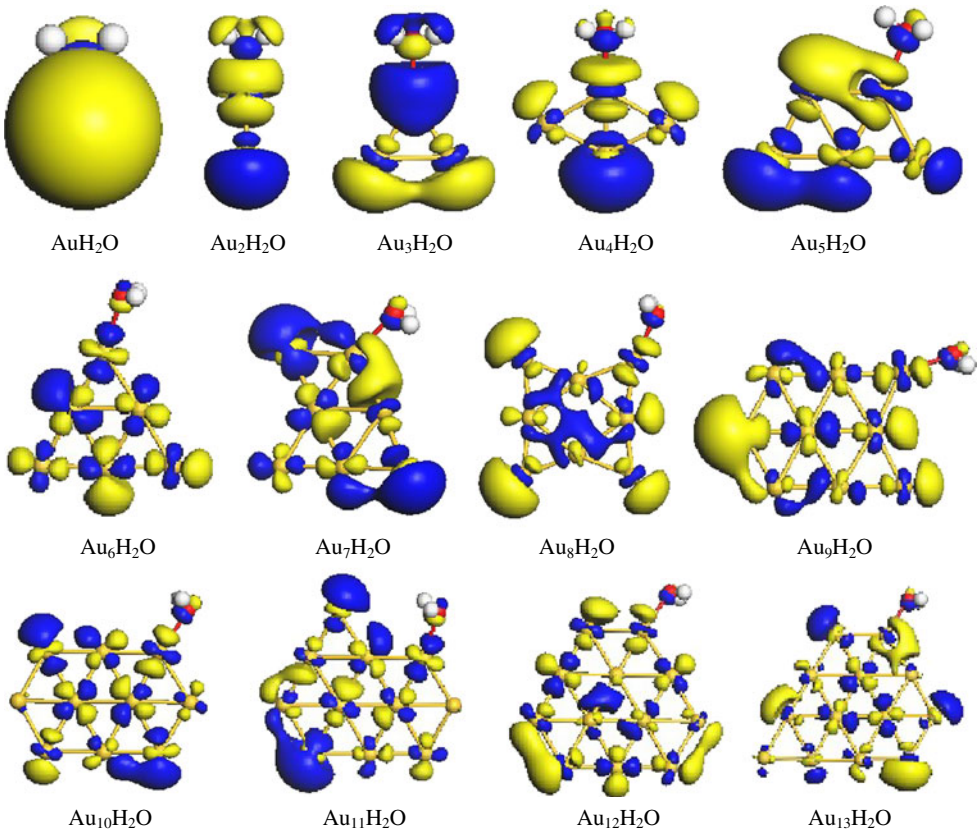

Fig. 6 Spatial orientations of HOMO for Au_nH2O (n=1-13) clusters

Magnetic properties

Finally, we will discuss the magnetic properties of Au_nH_2O clusters. From Table 3, we can see that all the Au_nH_2O clusters prefer low spin multiplicity (M=1 for even-numbered Au_nH_2O clusters, and M=2 for odd-numbered Au_nH_2O clusters). The even-numbered Au_nH_2O clusters are found to exhibit zero magnetic moment, and the odd-numbered Au_nH_2O clusters are found to possess a magnetic moment with the value of 1 μ_B (contributed mainly by Au_n). The odd-even alteration of magnetic moments for Au_nH_2O clusters is very obvious and may be served as a material with a tunable code capacity of "0" and "1" [48]. This situation can be simply understood by considering the electron pairing effect. Based on the valence electron configuration of Au6s^1, O2$s^2$2p^4 and H1s^1, respectively, as H_2O molecules are adsorbed onto even-numbered Au_n clusters, the even number of 6s electrons from the gold cluster and the even number of s, p electrons from the H_2O molecule prefer to form a closed electronic structure according to Hund's rule, so these Au_nH_2O clusters show zero magnetic moment according to Pauli repulsion in the case of the electron pairing. As a H_2O molecule is adsorbed onto an odd-numbered Au_n cluster, the odd number of 6 s electrons from the gold cluster and the even number of s, p electrons from the H_2O molecule prefer to form a open electronic structure according to Hund's rule, and possess a magnetic moment of 1μ_B with one unpaired electron. Previous studies [49–51] have shown that the charge transfer and hybridization of valence electrons stemming from the host, as well as impurities, influence the local magnetic moment significantly. The local magnetic moment of a scandium-doped gold system is quenched because of the strong pairing effect between the scandium 3d electrons and gold 6s electrons. This is similar to the situation of the pairing effect between the 6s electrons of the Au atom and the s, p electrons of the H_2O molecule in Au_nH_2O clusters in our work.

Considering all the factors mentioned above, we find that even-numbered Au_nH_2O clusters have larger adsorption energy, higher VIP, larger HLG, greater charge transfer, and stronger Au–O interactions compared with the adjacent odd-numbered Au_nH_2O clusters. The most favorable adsorption between small gold clusters and H_2O molecule seems to takes place when the H_2O molecule is adsorbed onto an even-numbered Au_n cluster and becomes a Au_nH_2O cluster with an even number of valence electrons. This situation can be explained in terms of the factors mentioned above, but the adsorption process cannot be explained equally based on these characteristics. Adsorption of an H_2O molecule onto a cluster with an even number of valence electrons can be seen to partly involve an excitation

of the formerly unoccupied orbital in the cluster, since the open shell has to be "pushed up" when the cluster–H_2O bond is formed. This situation does not occur in the case of H_2O molecule adsorption onto a cluster with odd number of valence electrons, where the net effect of the adsorption is that the formerly open cluster orbital becomes doubly occupied. The same argument can also be found in connection with the bond preparation method used in the cluster surface model [52].

Conclusions

In this paper, AER calculation on Au_nH_2O (n=1–13) clusters was performed using DFT with the generalized gradient approximation at PW91 level. The main conclusions can be summarized as follows:

(1) After adsorption, the small gold cluster would like to bond with oxygen, and the H_2O molecule prefers to occupy the single fold coordination site in all Au_n (n= 2–13) clusters. Reflecting the strong scalar relativistic effect, the Au_n geometries are distorted slightly but still maintain planar structures. The Au–Au bond is strengthened and the H–O bond is weakened, appearing as the shortening of Au–Au bond-length and the lengthening of H–O bond-length. The H–O–H bond angle becomes slightly larger. The reactivity enhancement of the H_2O molecule is obvious.

(2) The Au–O bond-lengths, adsorption energies, VIPs, HLGs, HOMO (LUMO) energy levels, charge transfers and the highest vibrational frequencies of the Au–O mode for Au_nH_2O clusters exhibit a clear odd-even oscillation. The most favorable adsorption between small gold cluster and H_2O molecule takes place when the H_2O molecule is adsorbed onto an even-numbered Au_n cluster and becomes Au_nH_2O cluster with an even number of valence electrons.

(3) The odd-even alteration of magnetic moments observed in Au_nH_2O clusters may serve as a material with a tunable code capacity of "0" and "1" by adsorbing a H_2O molecule onto an odd or even-numbered small gold cluster.

Acknowledgment This work is supported by the Nature Science Foundation of Chongqing city. No. CSTC - 2007BB4137.

References

1. Meng S, Wang EG, Gao SW (2004) Phys Rev B 69:195404–195416
2. Li JB, Zhu SL, Li Y, Wang FH (2007) Phys Rev B 76:235433–235440
3. Cho JH, Kleinman L (2002) Phys Rev B 66:113306–113309
4. Materzanini G, Tantardini GF, Lindan PJD, Saalfrank P (2005) Phys Rev B 71:155414–155430
5. Blanco R, Orts JM (2008) Electrochim Acta 53:7796–7804
6. Henderson MA (2002) Surf Sci Rep 46:1–308
7. Taylor CD, Neurock M (2005) Curr Opin Solid State Mater Sci 9:49–65
8. Clay C, Hodgson A (2005) Curr Opin Solid State Mater Sci 9:11–18
9. Suzuki Y, Yamashita K (2010) Chem Phys Lett 486:48–52
10. Prestianni A, Martorana A, Labat F, Ciofini I, Adamo C (2009) J Mol Struct Theochem 903:34–40
11. Padilla-Campos L (2008) J Mol Struct Theochem 851:15–21
12. Assadollahzadeh B, Schwerdtfeger P (2009) J Chem Phys 131:064306–064316
13. Kang GJ, Chen ZX, Li Z, He X (2009) J Chem Phys 130:034701–034706
14. Li GP, Hamilton IP (2006) Chem Phys Lett 420:474–479
15. Chrétien S, Buratto SK, Metiu H (2007) Curr Opin Solid State Mater Sci 11:62–75
16. Meier DC, Goodman DW (2004) J Am Chem Soc 126:1892–1899
17. Bernhardt TM (2005) Int J Mass Spectrom 243:1–29
18. Haruta M, Tsubota S, Kobayashi T, Kageyama H, Genet MJ, Delmon B (1993) J Catal 144:175–192
19. Boccuzzi F, Chiorino A, Manzoli M, Haruta M (2001) J Catal 202:256–267
20. Mul G, Zwijnenburg A, van der Linden B, Makkee M, Moulijn JA (2001) J Catal 201:128–137
21. Jia JF, Haraki K, Kondo JN, Domen K, Tamaru K (2000) J Phys Chem B 104:11153–11156
22. Sárkány A, Révay Z (2003) Appl Catal A:Gen 243:347–355
23. Ju SP (2005) J Chem Phys 122:094718–094723
24. Chang CI, Lee WJ, Young TF, Ju SP, Chang CW, Chen HL, Chang JG (2008) J Chem Phys 128:154703–154712
25. Weng MH, Lee WJ, Ju SP, Chao CH, Hsieh NK, Chang JG, Chen HL (2008) J Chem Phys 128:174705–174713
26. Choudhary TV, Goodman DW (2002) Top Catal 21:1–12
27. Fernandez EM, Soler JM, Garzon LL, Balbas C (2004) Phys Rev B 70:165403–165416
28. Orita H, Itoh N, Inada Y (2004) Chem Phys Lett 384:271–276
29. Lee YS, McLean AD (1982) J Chem Phys 76:735–736
30. Datta SN, Ewig CS (1982) Chem Phys Lett 85:443–446
31. Hakkinen H, Landman U (2000) Phys Rev B 62:R2287–R2290
32. Myoung H, Ge M, Sahu BR, Tarakeswar P, Kim KS (2003) J Chem Phys 107:9994–10002
33. Fernandez EM, Soler JM, Garzon LL, Balbas C (2004) Phys Rev B 70:165403–165416
34. Mao HP, Wang HY, Ni Y, Xu GL (2004) Acta Phys Sin 53:1766–1771
35. Deka A, Deka RC (2008) J Mol Struct Theochem 870:83–93
36. Hakkinen H, Yoon B, Landman U, Li X, Zhai HJ, Wang LS (2003) J Phys Chem A 107:6168–6175
37. Feller D, Glendening ED, de Jong WA (1999) J Chem Phys 110:1475–1491
38. Schröder D, Schwarz H, Hrušák J, Pyykkö P (1998) Inorg Chem 37:624–632
39. (1993-1994) In: Lide DR (ed) CRC Handbook of chemistry and physics. Chemical Rubber Company, Boca Raton, pp74–75
40. Cao ZX, Wang YJ, Zhu J, Wu W, Zhang Q (2002) J Phys Chem B106:9649–9654
41. Poater A, Duran M, Jaque P, Toro-Labbe A, Sola M (2006) J Phys Chem B 110:6526–6536
42. Ding XL, Li ZY, Yang JL, Hou JG, Zhu QS (2004) J Chem Phys 121:2558–2562

43. Wu X, Senapati L, Nayak SK, Selloni A, Hajaligol M (2002) J Chem Phys 117:4010–4015
44. Ghebriel HW, Kshirsagar A (2007) J Chem Phys 126:244705–244713
45. Phala S, Klatt G, Steen EV (2004) Chem Phys Lett 395:33–37
46. Eberhart ME, Handley RC, Johnson KH (1984) Phys Rev B 29:1097–1100
47. Ding XL, Li ZY, Yang JL, Hou JG, Zhu QS (2004) J Chem Phys 120:9594–9601
48. Zhang M, He LM, Zhao LX, Feng XJ, Cao W, Luo Y (2009) J Mol Struct Theochem 911:65–69
49. Torres M, Fernández E, Balbás L (2006) Phys Rev B 71:155412–155418
50. Majumder C, Kandalam A, Jena P (2006) Phys Rev B 74:205437–205442
51. Janssens E, Tanaka H, Neukermans S, Silverans RE, Lievens P (2004) Phys Rev B69:085402–085410
52. Panas I, Siegbahn P, Walhgren U (1987) Chem Phys 112:325–337